Bifunctionality of Rh3+ modifier on TiO2 and working mechanism of Rh3+/TiO2 photocatalyst under irradiation of visible light

*Sho Kitano,† Naoya Murakami,‡ Teruhisa Ohno,‡ Yasufumi Mitani,§ Yoshio Nosaka,§ Hiroyuki Asakura,¶ Kentaro Teramura,¶ Tsunehiro Tanaka,¶ Hiroaki Tada,# Keiji Hashimoto,# Hiroshi Kominami#,**

†Interdisciplinary Graduate School of Science and Engineering, Kinki University, 3-4-1 Kowakae, Higashiosaka, Osaka 577-8502, Japan.

‡Department of Applied Chemistry, Faculty of Engineering, Kyushu Institute of Technology, 1-1 Sensuicho, Tobata, Kitakyushu 804-8550, Japan.

§Department of Materials Science and Technology, Nagaoka University of Technology, Nagaoka 940-2188, Japan.

¶Department of Molecular Engineering, Graduate School of Engineering, Kyoto University, Kyoto 615-8510, Japan.

[#]Department of Applied Chemistry, Faculty of Science and Engineering, Kinki University, 3-4-1 Kowakae, Higashiosaka, Osaka 577-8502, Japan.

ABSTRACT: A rhodium(III) ion (Rh^{3+})-modified TiO_2 (Rh^{3+}/TiO_2) photocatalyst, prepared by a simple adsorption method and exhibiting high levels of photocatalytic activity in degradation of organic compounds, was investigated by using X-ray absorption fine structure (XAFS) measurements, (photo)electrochemical measurements, double-beam photoacoustic (DB-PA) spectroscopic measurements and photoluminescence measurements. Based on the results, the features of the Rh^{3+} modifier and the working mechanism of the Rh^{3+}/TiO_2 photocatalyst are discussed. XAFS measurements revealed that the Rh^{3+} species were highly dispersed and almost atomically isolated on TiO_2. The (photo)electrochemical measurements, DB-PA spectroscopic measurements and photoluminescence showed a unique bifunction of the Rh^{3+} modifier as a promoter for O_2 reductions and an electron injector to the conduction band of TiO_2 for response to visible light. The reasons for the Rh^{3+}/TiO_2 photocatalyst exhibiting higher levels of photocatalytic activity than those of TiO_2 photocatalysts modified with other metal ions are also discussed on the basis of obtained results.

1. Introduction

Titanium(IV) oxide (TiO_2) is an efficient photocatalyst that has strong oxidation abilities and widely used for many practical applications.[1-3] However, TiO_2 only works under irradiation of UV light due to its wide band gap, 3.2 eV (anatase), and many technologies have been developed

to make TiO_2 respond to visible light for efficient utilization of solar or indoor light.[4-22] Surface modification of TiO_2 with transition metals is one of the important methods to visualize TiO_2-based photocatalysts.[10-22] In this method, various transition metals are not doped in lattices but are just fixed on the surface of TiO_2, and charge transfers occur between the metals and TiO_2 under irradiation of visible light. These photocatalysts have flexibility and variation because there are many candidates of transition metals as modifiers, and properties of TiO_2 supports can be controlled to maximize photocatalytic activities in objective reactions.

Kisch *et al*. reported TiO_2 photocatalysts modified with inorganic sensitizers including platinum(IV) and rhodium(III) chlorides.[10, 11] These metal chloride-modified photocatalysts were prepared by the impregnation method using TiO_2 powders and metal sources followed by calcination for fixation. In platinum chloride-modified photocatalysts, a platinum chloride absorbs visible light and splits a Pt^{III} intermediate and a surface-bound chlorine atom due to homolytic Pt^{IV}-Cl bond cleavage. A Pt^{III} intermediate injects an electron into the conduction band of TiO_2 and a chlorine atom oxidizes substrates, and they return to initial states. In rhodium chloride-modified photocatalysts, a rhodium-to-titanium charge transfer transition (from a rhodium chloride to the conduction band of TiO_2) occurs under irradiation of visible light, and an electron injected in the conduction band and a Rh^{IV} center which oxidizes substrates are generated. The electrons in the conduction band are accepted by O_2.

Recently, TiO_2 photocatalysts modified with molecular metal oxide species introduced by using the chemisorption-calcination cycle (CCC) technique have been reported by one of authors of this paper.[12-14] In these photocatalysts, electronic excitation occurs from the surface d sub band to the conduction band of TiO_2 under irradiation of visible light, and the holes generated in the d sub band oxidized substrates, while the surface iron oxide species promote O_2 reduction.

Ohno and Murakami, also authors of this paper, have reported TiO_2photocatalysts modified with metal ions.[15] The photocatalysts were easily prepared by stirring a suspension of TiO_2 in a metal chloride solution followed by filtration and drying (*no heat treatment*). In these photocatalysts, metal ion species were probably fixed as metal oxides or hydroxide clusters. The metal ion species inject electrons into the conduction band of TiO_2 under irradiation of visible light and become an oxidative state that oxidizes substrates. The metal ion species also works as electron acceptors from the conduction band of TiO_2 like a cocatalyst.

On the other hand, a different working mechanism has been proposed by Irie *et al*. despite using a similar photocatalyst system.[16-18] They suggested that the interfacial charge transfer (IFCT) from the valence band of TiO2 to redox potentials of the metal ion species16-18 occurs under irradiation of visible light and that the holes generated in the valence band oxidize the substrates. The metal ion species that have accepted electrons reduce O_2molecules through multi-electron reduction and then return to the initial states.

These *modified* photocatalysts have been mainly used for mineralization of harmful organic compounds; however, it is expected that they can be applied to various other reactions due to their properties as described above. For application of these *modified* photocatalysts to various reactions, it is important to analyze and clarify their features in detail. Although the working mechanisms and features of these photocatalysts and the states of modifiers have been partially investigated using some measurements in the reports, there have been few reports on their detailed characterization.

Recently, we have developed a new photocatalyst responding to visible light, rhodium(III) ion-modified TiO_2 (Rh^{3+}/TiO_2). Modification of TiO_2 with Rh^{3+} was very simple; it was achieved only by adsorption from an Rh^{3+} solution and subsequent drying at a moderate temperature (*no*

calcination), resulting in small energy consumption in the preparation process. We have reported that this photocatalyst exhibited higher levels of activities than those of TiO_2 photocatalysts modified with other metal ions in mineralization of volatile organic compounds (VOC) under irradiation of visible light.[20-22] Results obtained in those studies indicate that the Rh^{3+}/TiO_2 photocatalyst works by a unique mechanism and that Rh species fixed on the surface of TiO_2 work as electron injectors or sensitizers for response to visible light. Comparable studies using anatase- and rutile-type TiO_2 have suggested that Rh species also act as promoters for O_2 reduction by electrons injected in the conduction band of TiO_2 similar to photocatalysts reported by Ohno *et al*.[15] However, the working mechanism and the reason why the Rh^{3+}/TiO_2 photocatalyst exhibits excellent photocatalytic activities are still unclear. In this study, we investigated functions of Rh species fixed on TiO_2 by using various methods such as X-ray absorption fine structure (XAFS) measurements, (photo)electrochemical measurements, double-beam photoacoustic (DB-PA) spectroscopic measurements and photoluminescence measurements. Based on the results, we discuss bifunctionality of Rh species fixed on TiO_2 and the working mechanism of the Rh^{3+}/TiO_2 photocatalyst under irradiation of visible light.

2. Experimental

2.1. Sample preparation

All of the chemicals were used as received without further purification. Semiconductor oxide supports, TiO_2, Ta_2O_5 and Nb_2O_5, were synthesized by the HyCOM (Hydrothermal Crystallization in Organic Media) method reported previously to obtain samples having a large specific surface area.[23-24] Commercial samples from Kanto Nanotek were used for SnO_2. HyCOM-TiO_2, HyCOM-Ta_2O_5 and SnO_2 powders were calcined at 550, 800 and 500^{o}C,

respectively, in a box furnace for 1 h. The samples were modified with Rh^{3+} by the equilibrium method.[20-22] The samples were added to an aqueous solution of rhodium(III) chloride, the charged amount of which corresponded to 1.0 wt% of Rh^{3+}, and stirred and heated in a water bath at *ca*. 90ºC. The suspension was filtered and the filtrate was washed repeatedly with distilled water and then the filtrate was dried *in vacuo* for 1 h. The amount of Rh^{3+} fixed on TiO_2 was determined by analysis of Rh^{3+} in the filtrate using inductively coupled plasma atomic emission spectroscopy (ICP-AES, Shimadzu ICPS-7500).

The Rh^{3+} species in the prepared samples were modified only on the surface of oxide supports since thermal treatment was not carried out after modification with Rh^{3+}, which is different from element-doped photocatalysts calcined at high temperature. Thus, the Rh^{3+} species did not exist in the bulk of supports like dopants, often working as recombination centers. In addition, most of the chloride, which is generally thought to be a cause of deactivation, on the prepared samples was eliminated by elaborate washing.

2.2. Characterization

Powder X-ray diffraction (XRD) was measured using Cu$K\alpha$ radiation by a Rigaku MultiFlex equipped with a carbon monochromator. Specific surface area (S_{BET}) of the samples was measured using the Brunauer-Emmett-Teller (BET) single-point method on the basis of nitrogen (N_2) uptake measured at -196ºC using a Shimadzu Flowsorb 2300. Diffuse reflectance spectra of the samples were measured using a Shimadzu UV-2400 UV-Vis spectrometer equipped with a diffuse reflectance measurement unit (ISR-2000) and recorded after Kubelka–Munk analysis. Rh K-edge XAFS spectra of the as-prepared Rh^{3+}/TiO_2 photocatalyst and reference samples (Rh foil and Rh_2O_3) were recorded at the BL01B1 beamline at the SPring-8 (Japan Synchrotron

Radiation Research Institute, Hyogo, Japan) in the transmission mode for Rh foil and Rh_2O_3 and fluorescence mode for Rh^{3+}/TiO_2 samples at ambient temperature. An Si (311) two-crystal monochromator was used to obtain a monochromatic X-ray beam. The photon energy was calibrated at the inflection point of the absorption edge of an X-ray absorption near edge structure (XANES) spectrum of Rh foil. Higher harmonics were removed by slight detuning of the monochromator. Data reduction was carried out with Athena and Artemis included in the Ifeffit package.

The features of Rh^{3+} were analyzed by electrical measurement. A slurry of HyCOM-TiO_2 particles (HyCOM-TiO_2 0.05 g/ethylene glycol 0.01 ml) was coated on conductive glass (F-doped SnO_2, 10 Ω/cm^2) by a squeegee method, and the electrode was heated at 823 K for 1 h, and then the HyCOM-TiO_2 electrode was modified with Rh^{3+} by the same method as that described above. Photocurrent and current-potential curves of the electrodes were measured in a 0.1 M-$NaClO_4$ electrolyte solution in a regular three-electrode electrochemical cell on a galvanostat/potentiostat (HZ-5000, Hokuto Denko) under atmosphere. A Xe lamp with a Y-43 cut filter (85 mW cm^{-2}, 400 - 600 nm) was used as the source of visible light. Glassy carbon and an Ag/AgCl electrode (TOA-DKK) were used as the counter electrode and reference electrode, respectively.

The behaviors of electrons on samples in gas phase were analyzed by DB-PA spectroscopic measurements. A gas-exchangeable photoacoustic cell equipped with two valves for gas flow was used, and a sample was placed in the cell. The atmosphere was controlled by a flow of artificial air or N_2 containing ethanol vapor (air + EtOH, N_2 + EtOH), and the measurements were conducted after shutting off the valves, i.e., in a closed system at room temperature. An LED emitting light at ca. 625 nm (Luxeon LXHL-ND98) was used as a probe light, and the

output intensity was modulated by a digital function generator (NF DF1905) at 80 Hz. In addition to the modulated light, a UV-LED (Nichia NCCU033, 365 nm, 1.6 mW cm^{-1}) and a blue LED (Luxeon LXHL-NB98, 470 nm, 3.6 mW cm^{-1}) were also used as simultaneous continuous irradiation for photoexcitation of samples. The PA signal acquired by a condenser microphone buried in the cell was amplified and monitored by a digital lock-in amplifier (NF LI5640). Detailed setups of DB-PA spectroscopic measurements have been reported.[25]

Active oxygen species formed in reactions using an Rh^{3+}/TiO_2 photocatalyst were measured by chemiluminescence (CL) photometry.[26-29] The formation of $O_2^{\bullet-}$ was observed by using a luminol CL probe method. A quartz cell (1 cm-1 cm) containing a photocatalyst (15 mg) suspension in 3.5 mL of 0.01 M NaOH solution was placed in a dark box and irradiated with a 14 mW He-Cd laser (KIMMON, IK5652R-G) at the wavelength of 442 nm. Immediately after the laser irradiation, 50 μL of 7 mM luminal solution was injected via a microsyringe into the irradiated suspension. The CL intensity was measured with a Peltier-cooled photon counter head (Hamamatsu, H7421), and number of photons counted was integrated over 100 s. Other details of the apparatus and the CL reaction have been reported previously.[27] The experimental procedure for the selective detection of H_2O_2 is basically the same as the O_2 •− measurement except for the injection solution and the timing. The suspension was mounted in the dark box in the same place as that for the $O_2^{\bullet-}$ measurement. After irradiation of the photocatalysts, the suspension was kept in the dark for 30 min for elimination of $O_2^{\bullet-}$, and then 50 μL of 7 mM luminol solution (0.01 M NaOH) was added. The suspension containing luminol was kept again for 10 min in the dark. Then 50 μL of hemoglobin (Hb) solution was injected via a microsyringe into the suspension and the time profile of CL intensity was measured repeatedly. To convert the observed CL intensities to the absolute concentrations of $O_2^{\bullet-}$ and H_2O_2, the

apparatus factor was calculated from the experiment in which all luminal molecules are consumed for the reaction with an excess amount of H_2O_2.

2.3. Evaluation of photocatalytic activity under irradiation of visible light

A sample (30 mg) was suspended in a small amount of distilled water and then the powder was spread on a glass filter (GF-75, 26 mm in diameter, Advantec) with a Buchner funnel under suction. The glass filter together with the sample was dried *in vacuo* for 1 h. he glass filter together with the sample and a glass vessel containing an aqueous solution of acetone (1 vol%) were placed in a glass reactor. The gas phase in the system was replaced with artificial air (oxygen (O_2) (20%)-nitrogen (N_2) gas mixture), and acetone was gradually evaporated and then the vapor was saturated in the reactor. After adsorption of acetone had reached an equilibrium, the photocatalyst was irradiated by visible light or UV light, of which the intensities on the surface of the glass filter were 95 mW cm^{-2} (400-600 nm) and 120 mW cm^{-2} (300-450 nm), respectively. The amounts of acetone and CO_2 were determined by a gas chromatograph (Agilent Technologies, A3000 micro GC).

3. Results and discussion

3.1. XAFS analysis for state of Rh species on the surface of TiO_2

In previous studies,[20-22] we investigated activities of Rh^{3+}/TiO_2 photocatalysts and the effect(s) of physical properties of TiO_2 samples on the activities. However, states of Rh species fixed on TiO_2 were hardly investigated. Here, the states and the surrounding condition of Rh species were analyzed by XAFS measurements.

Figure 1A shows Rh K-edge XANES spectra of Rh foil, rhodium(III) oxide (Rh_2O_3) and Rh3+/TiO2 samples. Figure 1B shows an enlargement of XANES spectra in Figure 1A. The spectrum of the Rh^{3+}+/ TiO_2 sample was similar to that of Rh_2O_3 but different from that of Rh foil. The absorption edge energy of Rh species of Rh^{3+}+/ TiO_2 (23 215.5 eV) is comparable to that of Rh_2O_3 (23 215.2 eV), indicating that the oxidation state of Rh species of Rh^{3+}+/ TiO_2 is trivalent. Figure 2 shows Fourier transforms (FT) of k^3-weighted Rh K-edge EXAFS spectra of Rh_2O_3 and Rh^{3+}/TiO_2 samples. The Fourier-transformed spectrum of Rh_2O_3 shows three peaks at around 1.60, 2.64, and 3.34 Å, which are attributed to the scatterings by Rh-O and a couple of Rh-Rh shells, respectively. However, the Fourier-transformed spectrum of Rh^{3+}/TiO_2 exhibits only a single peak at 1.60 Å, which is due to the Rh-O shell. he clear difference in spectral features strongly suggests that the Rh^{3+} species are highly dispersed and almost atomically isolated on TiO2.

This is clearly different from Cu and Fe species reported by Irie and coworkers, which were grafted as amorphous oxyhydroxide clusters on TiO_2.[17, 18] The isolated Rh^{3+} was probably modified as a complex-like form coordinated by the surface hydroxyl group of TiO_2 and H_2O since we confirmed that chlorides were almost completely eliminated by washing with distilled water in the preparation.

3.2. Electrochemical measurements under irradiation of visible light and in the dark

Electrochemical measurements were used to investigate the behavior of electrons in Rh^{3+}/TiO_2 under irradiation of visible light and in the dark. Based on the results obtained, the role(s) of Rh^{3+} will be discussed. Figure 3 shows time courses of photocurrent measurements of bare TiO_2 and Rh^{3+}/TiO_2 electrodes under irradiation of visible light. A photocurrent was hardly

observed in the bare TiO_2 electrode, indicating that band-gap excitation of TiO_2 was negligible under the present irradiation conditions. On the other hand, a large anodic photocurrent was observed when the Rh^{3+}/TiO_2 electrode was used. The observed anodic current means that electrons transferred from the working electrode to the counter electrode through the circuit.

These results for the bare TiO_2 and Rh^{3+}/TiO_2 electrodes suggest that electrons transferred from Rh^{3+} to the conduction band of TiO_2 in the latter electrode under irradiation of visible light. The photocurrent decreased in the initial stage. However, thereafter a stable constant photocurrent was observed, indicating that Rh^{3+} fixed on TiO_2 works as a stable electron injector.

Figure 4 shows current (*I*, milliamps)-potential (*E*, plots vs. NHE) curves of the bare TiO_2 and Rh^{3+}/TiO_2 electrodes in the dark in the presence of air. A current was hardly observed in the absence of O_2 in both electrodes. In the case of the bare TiO_2 electrode in the presence of air, the current did not flow at the potential range between 0 and 0.4 V. Below 0 V, a small current due to O_2 reduction was observed. This current corresponded to one-electron reduction of O_2 ($O_2 + H^+ + e^- = HO_2$, $E^0 = -0.046$ V). [30] On the other hand, a larger current of O_2 reduction was observed when the Rh^{3+}/TiO_2 electrode was used. These results indicate that Rh^{3+} fixed on the surface of TiO_2 greatly promoted electron transfer from TiO_2 to O_2 molecules. It should be noted that the potential at which the current started to flow shifted toward the positive region (ca. 0.15 V) in the case of the Rh^{3+}/TiO_2 electrode. This potential is in good agreement with the redox potentials of Rh^{3+} ($Rh^{3+} + e^- = Rh^{2+}$, $E^0 = 0.158$ V; $Rh^{3+} + 2e^- = Rh^+$, $E^0 = 0.158$ V).[30] At this potential, multi-electron reductions of O_2 (two-electron reduction: $O_2 + 2H^+ + 2e^- = H_2O_2$, $E^0 = 0.68$ V; or four-electron reduction: $O_2 + 4H^+ + 4e^- = 2H_2O$, $E^0 = 1.23$ V)[30] are possible because the redox potential of Rh^{3+} is more positive than that of one-electron reduction of O_2 and more negative than that of multi-electron reductions of O_2. Therefore, it can be concluded from the

electrochemical behaviors of the bare TiO_2 and Rh^{3+}/TiO_2 electrodes in the dark that the Rh^{3+} species accepted electrons from TiO_2 at 0.158 V, resulting in the formation of reduced Rh species (Rh^{2+} or Rh^{+}) and that the reduced Rh species transferred electrons to O_2 molecules through their multi-electron reductions. Active oxygen species formed by reduction of O_2 molecules in the Rh^{3+}/TiO_2 suspension system were also investigated and will be discussed later (section 3.5).

3.3. DB-PA spectroscopic measurement under irradiation of UV or visible light

DB-PA spectroscopic measurement enables detection of electrons in the conduction band of TiO_2 by detection of trivalent titanium (Ti^{3+}) species reduced.[15, 25] Thus, behaviors of electrons in samples during reactions can be directly analyzed by the DB-PA spectroscopic measurement. Electrochemical measurements enable accurate analysis of redox potentials and electrical properties of samples. However, electrochemical measurements indicate reactions occurring between molecules and the electrode in the *solid-liquid* interface. ince Rh^{3+}/TiO_2 photocatalysts were used for degradation of VOC, the photocatalysts were set in air containing VOC.[20-22] Therefore, the behaviors of Rh species and/or electrons in the *solid-gas* interface should also be evaluated. In this sense, the DB-PA spectroscopic measurement is important to understand the behaviors of Rh species and/or electrons in Rh^{3+}/TiO_2 in the solid-gas photocatalytic reaction. Figure 5 shows time courses of PA signals of bare TiO_2 and Rh^{3+}/TiO_2 samples under irradiation of visible light from a blue LED in the presence of N_2 and ethanol (deaerated condition). Under this condition, holes in the valence band of TiO_2 are consumed by ethanol, while electrons in the conduction band accumulate because of the absence of appropriate electron acceptors such as O_2 molecules. The PA signal of the bare TiO_2 sample did not

increase, indicating that no band gap excitation in TiO occurred under irradiation of visible light. Meanwhile, the PA signal of the Rh^{3+}/TiO_2 sample gradually increased. This result shows that electron transfer in the Rh^{3+}/TiO_2 sample and accumulation of electrons in TiO_2 (formation of Ti^{3+}) occurred under visible light irradiation in the absence of O_2. Formation of Ti^{3+} was helpful for determining the path of photoexcitation, i.e., formation of Ti^{3+} means that electrons transferred to the conduction band of TiO_2 by irradiation of visible light. Taking into account the band-gap of TiO_2, energy of visible light irradiated and the results for photoelectrochemical response of the Rh^{3+}/TiO_2 electrode, we can conclude that the response of Rh^{3+}/TiO_2 to visible light originated from the charge transfer from Rh^{3+} to the conduction band of TiO_2.

Figure 6 shows time courses of PA signals of bare TiO_2 and Rh^{3+}/TiO_2 samples under irradiation of UV light in the presence of artificial air (N_2:O_2 = 80:20) and ethanol. In this condition, electrons generated in the conduction band by band-gap excitation under irradiation of UV light were consumed by reduction of O_2 molecules. Thus, O_2 reduction ability of samples at the gas-solid interface was evaluated using this PA method. The signal does not increase if the excited electrons immediately transfer to O_2 molecules. The PA signal of bare TiO_2 steeply increased and was gradually saturated, indicating that accumulation of electrons occurred due to relatively slow consumption of electrons, i.e., reduction of O_2, and then accumulation and consumption of electrons tended to reach an equilibrium with prolongation of irradiation. On the other hand, the PA signal of Rh^{3+}/TiO_2 was almost unchanged before and after irradiation of UV light. This result indicates that electrons excited to the conduction band by UV irradiation immediately transferred to O_2; i.e., the reduction of O_2 was drastically promoted by Rh^{3+} as was observed in electrochemical measurement (Figure 4). It has been reported that PA signals of various TiO_2 samples modified with other metal ions also decreased compared to that of bare

TiO_2 , under the almost same condition of this report.[15] It should be noted that a small signal was observed in the case of TiO_2 samples modified with other metal ions, whereas a signal of Rh^{3+}/TiO_2 was hardly observed, indicating that Rh^{3+} has a higher level of O_2 reduction ability than that of other metal ions. Therefore, from the results of electrochemical and DB-PA spectroscopic measurements, we can conclude that Rh^{3+} fixed on Ti effectively works as a promoter for the reduction of O_2.

3.4. Investigation of the mechanism of charge transfer from Rh^{3+} to the conduction band of supports

Results of photoelectrochemical analysis and PAS revealed that electrons were injected from Rh species to the conduction band of TiO_2 under irradiation of visible light. However, the results are not sufficient to clarify the excitation mechanism since two excitation routes have been revealed in several studies: 1) indirect charge transfer in which electrons in Rh^{3+} are excited and then move to the conduction band of TiO_2 like a sensitizer system[10] as shown in Figure 7(A) and 2) direct charge transfer from Rh^{3+} to the conduction band of TiO_2 as shown in Figure 7(B). For investigating which charge transfer occurs, some semiconductor oxides having various energy levels of the conduction band were modified with Rh^{3+} and the photocatalytic activity of the samples was evaluated using decomposition of VOC in gas phase under irradiation of visible or UV light. Some semiconductor metal oxides were synthesized by HyCOM methods[23, 24] giving nanocrystalline metal oxides with a large specific surface area that is suitable for modification with a large amount of Rh^{3+} and thus enabling clear observation of the effect of Rh^{3+} modification.

Table 1 shows the physical properties of various metal oxides. The metal oxides have band gaps larger than that of TiO_2, indicating that they do not respond to visible light. Figure 8(A) shows diffuse reflection spectra of bare metal oxides and emission spectra of visible light and UV light. All samples showed photoabsorption corresponding to their band-gap excitations. The SnO_2 sample also showed a shoulder in the visible light region due to oxygen vacancies, which did not contribute to the photocatalytic activity under irradiation of visible light. Figure 8(B) shows diffuse reflection spectra of Rh^{3+}-modified samples and emission spectra of visible and UV light. All modified samples exhibited additional photoabsorption in a longer wavelength region. The photoabsorption in the range around 450 nm originated from *d-d* transition of Rh, $^1A_{1g} \rightarrow {}^2T_{2g}$ [11, 33] The photoabsorption in the range from visible to UV light regions probably originated from the charge transfer from Rh^{3+} to the conduction band of semiconductors, which depends on the semiconductor oxide.

Figure 9 shows rates of CO_2 formation in decomposition of gaseous acetone, a VOC, over the Rh^{3+}-modified samples under irradiation of visible light from the blue LED. No CO_2 was formed over any of the bare samples due to insufficient energy of the blue light for band-gap excitation of the semiconductors. The Rh^{3+}-modified TiO_2, Nb_2O_5, and SnO_2 samples exhibited photocatalytic activity for degradation of acetone, whereas the Rh^{3+}-modified Ta_2O_5 sample did not.dThese results indicate that the charge transfer from Rh^{3+} to the conduction band of the semiconductors by visible light occurs only when the energy levels of the conduction bands of the semiconductors are located close to or below that of the conduction band of TiO_2. Figure 10 shows the rates of CO_2 formation for decomposition of gaseous acetone over bare and Rh^{3+}-modified Ta_2O_5 samples under irradiation of UV light.dThe bare Ta_2O_5 sample showed almost no photocatalytic activity, indicating that the energy required for the band-gap excitation of

Ta_2O_5 was slightly larger than that of UV light irradiated. On the other hand, acetone was mineralized over Rh^{3+}-modified Ta_2O_5 under UV irradiation, indicating that another route for charge separation was created by modification of Ta_2O_5 with Rh^{3+}. If the route created by modification of Ta_2O_5 with Rh^{3+} is the indirect charge transfer route, the Rh^{3+}-modified Ta_2O_5 sample would not exhibit photocatalytic activity under irradiation of UV light because the energy required for excitation of the Rh^{3+} species and indirect charge transfer do not depend on the type of semiconductors in experiments on visible light excitation. If the direct route from Rh^{3+} to the conduction band of Ta_2O_5 is created, whether the charge transfer occurs or not should depend on the energy of light irradiated to Rh^{3+}-modified Ta_2O_5. Experimental results for photocatalytic activity of Rh^{3+}-modified Ta O indicate that the excitation of electrons occurred via direct charge transfer from Rh^{3+} to the conduction band of Ta_2O_5. In addition, it was supported by the fact that the absorption due to the charge transfer depends on the semiconductors as shown in Figure 8(B). Therefore, it can be concluded that charge separation in Rh^{3+}-modified semiconductor photocatalysts under irradiation of light occurred directly from Rh^{3+} to the conduction band of semiconductors.

The photocatalytic activities of these samples cannot be easily compared since the physical properties of supports, the amount of Rh^{3+} modified and further factors of the samples were not optimized. The effects of supports on the photocatalytic activity of Rh^{3+}-modified photocatalysts will be reported separately.

3.5. Investigation of active oxygen under irradiation of visible light

The bifunction of Rh^{3+} was discussed in previous sections. However, it is important to clarify not only the behaviors of electrons in the Rh^{3+}/TiO_2 photocatalyst but also active oxygen species

formed by Rh^{3+}/TiO_2 because the latter information would reveal the whole working mechanism including interactions between the Rh^{3+}/TiO_2 photocatalyst and oxygen molecules. Thus, CL photometry was carried out for investigation of active oxygen species produced by photocatalysis of Rh^{3+}/TiO_2 under irradiation of visible light.

Figure 11 shows time courses of $O_2^{\bullet-}$ and H_2O_2 formed by Rh^{3+}/TiO_2 under irradiation of visible light. The Rh^{3+}/TiO_2 photocatalyst produced H_2O_2 under irradiation of visible light, indicating that Rh^{3+} on TiO_2 obviously worked as a co-catalyst for formation of H_2O_2 through two-electron reduction of O_2. Moreover, the amount of H_2O_2 formed by Rh^{3+}/TiO_2 was much larger than that of H_2O_2 formed by a Cu^{2+}-grafted TiO_2 photocatalyst (less than 1 nM) reported previously under the same condition of this report.[29] This result indicates that Rh^{3+} possesses higher activity than that of Cu^{2+} in multi-electron reduction of O_2.

The Rh_3+/TiO_2 photocatalyst also formed a very large amount of $O_2^{\bullet-}$ and the concentration reached a steady value around 200 nM. This amount was larger than that formed by other photocatalysts responding to visible light, *i,e.,* doped TiO_2 photocatalysts (nitrogen-doped TiO_2: 180 nM, sulfur-doped TiO_2: 70 nM).[28] In the Rh^{3+}/TiO_2 sample, one-electron reduction of O_2 occurred by direct migration of electrons from the conduction band of TiO_2 to O_2 molecules since anatase-type TiO_2 was used as a support for Rh^{3+}. The potential of the conduction band of anatase-type TiO_2, i.e., -0.2 V (vs NHE),[31, 32] is higher than the redox potential of one-electron reduction of O_2. In doped TiO_2 photocatalysts, nitrogen or sulfur are substituted to lattice atoms in the bulk of TiO_2, resulting in insertion of energy levels of the dopant in the forbidden band of TiO_2 and response to visible light due to excitation from the inserted energy level to the conduction band. However, the dopants often work as recombination sites, which decrease the photocatalytic performance. On the other hand, Rh^{3+} probably does not work as recombination

site since Rh^{3+} was not doped in bulk but just fixed on the surface of TiO_2 in the Rh^{3+}/TiO_2 photocatalyst. In this sense, modification with Rh^{3+} would be more advantageous than doping ions to prepare visible-light-responding photocatalysts using TiO_2.

The results of CL photometry clarified that Rh^{3+}/TiO_2 produced both H_2O_2 and $O_2^{\bullet-}$ through two- and one-electron reduction of O_2, respectively. The concentrations of H_2O_2 and $O_2^{\bullet-}$ were much larger than those of H_2O_2 and $O_2^{\bullet-}$ formed by other photocatalysts responding to visible light, Cu^{2+}-grafted TiO_2 and doped photocatalysts. It is interesting that the redox potentials of Rh^{3+} to Rh^{2+} and Rh^{+} are the same ($E^0 = 0.158$ V) as discussed in section 3.2, indicating that Rh^{2+} is unstable. Therefore, it is generally expected that two-electron reduction of Rh^{3+} to Rh^{+} easily occurs. This means that two-electron reduction of an O_2 molecule is possible at an Rh^{+} species ($O_2 + Rh^{+} + 2H^{+} = H_2O_2 + Rh^{3+}$). In the case of the Cu co-catalyst system, double amounts of the reduced Cu species are required to achieve two-electron reduction of an O_2 molecule (O2 + 2Cu+ + 2H+ = H2O2 + 2Cu2+) because the Cu+ −Cu2+ redox system only provides one electron. Therefore, a binuclear structure of Cu species would be required for two-electron reduction of O_2 molecules by the Cu co-catalyst system. In fact, Irie *et al*. reported that oxyhydroxide clusters were formed on the TiO_2 surface in a Cu/TiO_2 photocatalyst.[17] On the other hand, no binuclear structure would be necessary for the Rh^{3+}/TiO_2 photocatalyst because two-electron reduction of one O_2 molecule is possible at one Rh^{+} species. As shown in Figure 2, Rh species were fixed on the surface of TiO_2 in an isolated dispersion, indicating that there is almost no binuclear structure of Rh species on TiO_2 in the Rh^{3+}/TiO_2 photocatalyst. This structural result is in good agreement with both electrochemical properties of Rh species and reduction behavior of O_2 molecules over the Rh^{3+}/TiO_2 photocatalyst.

3.6. Working mechanism of Rh^{3+}/TiO_2 photocatalyst and features of bifunctional Rh^{3+}

Results obtained by XAFS measurments, electrochemical measurements, DB-PA spectroscopic measurements, CL photometry and photocatalytic reactions suggest the working mechanism of the Rh^{3+}/TiO_2 photocatalyst and the roles of Rh^{3+} shown in Figure 12. Under irradiation of visible light, Rh^{3+} directly injects electrons into the conduction band of TiO_2. The formed Rh species having a higher oxidation state oxidize substrates and return to the initial and stable oxidation state. Electrons injected to the conduction band move and some of them directly transfer to O_2 molecules through one-electron reduction and then $O_2^{\bullet-}$ molecules are formed, and the others are accepted by other Rh^{3+} and then reduced Rh species i.e., Rh^{+}, are formed. The reduced Rh species rapidly reduce O_2 molecules through multi-electron reduction and return to the trivalent state, and H_2O_2 (two-electron reduction) is mainly formed. Therefore, Rh^{3+} can work as a bifunctional modifier: as an electron donor under irradiation of visible light and as a promoter for multi−electron reduction of O_2. All of the Rh^{3+} species fixed on TiO_2 may not act as both electron injectors and promoters for O_2 reduction. It is known that TiO_2 has particular crystal faces on which oxidation or reduction preferentially proceeds.[34, 35] The role of Rh^{3+} might depend on crystal faces on which the Rh species were fixed and Rh^{3+} might work as either a promoter of O_2 reduction or an electron injector. However, it is clear from results obtained by various methods that Rh species possess both functions.

In mineralization of organic substrates over the Rh^{3+}/TiO_2 photocatalyst under irradiation of visible light, it is thought that oxidative decomposition of substrates is mainly performed by photoexcited Rh species having a higher oxidative state rather than by active oxygen species. From the results of XAFS measurements, the Rh^{3+} was fixed in an almost atomically isolated state, whereas Cu^{2+} and Fe^{3+} on TiO_2 were loaded in cluster forms as reported previously.[16-18]

Thus, the Rh^{3+}/TiO_2 photocatalyst has many active sites for both electron injection and oxidation of organic compounds (acetone in this study). It is interesting that the highest level of activity was obtained when the surface density of Rh^{3+} was 0.65 nm^{-2} (Figure S1). These many active sites are one of the reasons for high levels of activity of the Rh^{3+}/TiO_2 photocatalyst. In fact, Cu^{2+} and Fe^{3+}-grafted TiO_2 samples prepared as previously reported[18] exhibited the lower levels of activity (0.33 and 0.21 μmol h^{-1}) than that of Rh^{3+}/TiO_2 (2.2 μmol h^{-1}) in this evaluation as described in section 3.4. In addition, Rh^{3+} species work as single sites for two-electron reduction of O_2 because of the redox between Rh^{3+} and Rh^{+}. For Cu^{2+} and Fe^{3+}, two or more ions must contribute to the two-electron reduction as described in section 3.5. The optimum surface densities of Cu^{2+} and Fe^{3+} were reported to be 2.6 and 1.5 nm^{-2}, respectively.[18] The fact that the optimum density of Rh^{3+} (0.65 nm^{-2}) is smaller than those of Cu^{2+} and Fe^{3+} also suggests that a single site structure was formed in the Rh^{3+}/TiO_2 photocatalyst. The single site structure of the Rh^{3+}/TiO_2 photocatalyst is attributed to its effective H_2O_2 formation compared with Cu^{2+}-grafted TiO_2.[29] Therefore, the excellent properties of Rh^{3+} both as a promoter for O_2 reduction and an electron injector under irradiation of visible light resulted in higher levels of photocatalytic activity of the Rh^{3+}/TiO_2 photocatalyst than those of other photocatalyst responding to visible light.

Taken together, the results revealed that the Rh^{3+}/TiO_2 photocatalyst has unique features that other *modified* photocatalysts do not have. It is expected that the photocatalyst can be applied not only for oxidative decomposition of VOC but also for various photocatalyst systems. A study of reaction systems in which the Rh^{3+}/TiO_2 photocatalyst exhibits good photocatalytic activities is in progress.

4. Conclusions

The working mechanism of the Rh^{3+}/TiO_2 photocatalyst and features of the Rh^{3+} modifier were investigated by various methods. The XAFS measurements revealed that the Rh species have a trivalent state and are highly dispersed with an almost atomically isolated state on TiO_2.

(Photo)electrochemical measurements, DB-PA spectroscopic measurements and photoluminescence measurements showed that Rh^{3+} works as a bifunctional modifier, i.e., a electron injector for response to visible light and the promoter for multi-electron reduction of O_2. The Rh^{3+}/TiO_2 photocatalyst has many active sites due to the isolated dispersion of Rh^{3+}, which is different from Cu^{2+} and Fe^{3+} on TiO_2 photocatalysts consisting of cluster forms. In addition, Rh^{3+} species are capable of working as single sites for two-electron reduction of O_2 because of the redox between Rh^{3+} and Rh^{+} in contrast to the one-electron redox of Cu^{2+}-Cu^{+} and Fe^{3+}-Fe^{2+}. Therefore, these excellent and unique properties of Rh^{3+} as a bifunctional modifier resulted in higher levels of photocatalytic activities of the Rh^{3+}/TiO_2 photocatalyst than those of other photocatalysts responding to visible light.

ASSCIATED CONTENT

Supporting Information. Figure S1. This material is available free of charge via the Internet at http://pubs.acs.org.

AUTHOR INFORMATION

Corresponding Author

*E-mail address: hiro@apch.kindai.ac.jp (H. Kominami)

Present Addresses

†Hiroyuki Asakura, Synchrotron Radiation Research Center, Nagoya University, Furo-cho, Chikusa-ku, Nagoya 464-8603, Japan

ACKNOWLEDGMENT

This work was partly supported by a fund (Project No. P07020) from the Environmental Technology Development Department of New Energy and Industrial Technology Development Organization (NEDO). One of the authors (S. K.) appreciates the Japan Society for the Promotion of Science (JSPS) for a Research Fellowship for young scientists. One of the authors (H. K.) is also grateful for financial support from the Faculty of Science and Engineering, Kinki University.

REFERCNCES

(1) Matsuda, S.; Kato, A. *Appl. Catal.* **1983**, *8*, 149-165.

(2) Inomata, M.; Miyamoto, A.; Murakami, Y. *J. Chem. Soc., Chem. Commun.* **1980**, 233-234.

(3) Luck, F. *Bull. Soc. Chim. Belg.* **1991**, *100*, 781-800.

(4) Sato, S. *Chem. Phys. Lett.* **1986**, *123*, 126-128.

(5) Asahi, R.; Morikawa, T.; Ohwaki, T.; Aoki, K.; Taga, Y. *Science* **2001**, *293*, 269-271.

(6) Ohno, T.; Akiyoshi, M.; Umebayashi, T.; Asai, K.; Mitui, T.; Matsumura, M. *Appl. Catal. A* **2004**, *265*, 115-121.

(7) Anpo, M. *Catal. Surv. Jpn.* **1997**, *1*, 169-179.

(8) Abe, R.; Takami, H.; Murakami, N.; Ohtani, B. *J. Am. Chem. Soc.* **2008**, *130*, 7780-7781.

(9) Yu, H.; Irie, H.; Hashimoto, K. *J. Am. Chem. Soc.* **2010**, *132*, 6898-6899.

(10) Kisch, H.; Zang, L.; Lange, C.; Maier, F. W.; Antonius, C.; Meissner, D. *Angew. Chem. Int. Ed. Engl.* **1998**, *37*, 3034-3036.

(11) Dai, Z.; Burgeth, G.; Parrino, F.; Kisch, H. *J. Organomet. Chem.* **2009**, *694*, 1049-1054.

(12) Tada, H.; Jin, Q.; Nishijima, H.; Yamamoto, H.; Fujishima, M.; Okuoka, S.; Hattori, T.; Sumida, Y.; Kobayashi, H. *Angew. Chem. Int. Ed. Engl.* **2011**, *50*, 3501-3505.

(13) Jin, Q.; Fujishima, M.; Tada, H. *J. Phys. Chem. C* **2011**, *115*, 6478-6483.

(14) Jin, Q.; Ikeda, T.; Fujishima, M.; Tada, H. *Chem. Commun.* **2011**, *47*, 8814-8816.

(15) Murakami, N.; Chiyoya, T.; Tsubota, T.; Ohno, T. *Appl. Catal. A* **2008**, *348*, 148-152.

(16) Irie, H.; Miura, S; Kamiya, K.; Hashimoto, K. *Chem. Phys. Lett.* **2008**, *457*, 202-205.

(17) Irie, H.; Kamiya, K.; Shibanuma, T.; Miura, S.; Tryk, A. D.; Yokoyama, T.; Hashimoto, K. *J. Phys. Chem. C* **2009**, *113*, 10761-10766.

(18) Yu, H.; Irie, H.; Shimodaira, Y.; Hosogi, Y.; Kuroda, Y.; Miyauchi, M.; Hashimoto, K. *J. Phys. Chem. C* **2010**, *114*, 16481-16487.

(19) Irie, H.; Shibanuma, T.; Kamiya, K.; Miura, S.; Yokoyama, T.; Hashimoto, K. *Appl. Catal. B: Environ.* **2010**, *96*, 142-147.

(20) Kitano, S. Hashimoto, K. Kominami, H. *Chem. Lett.* **2010**, *39*, 627-629.

(21) Kitano, S.; Hashimoto, K.; Kominami, H. *Appl. Catal. B: Environ.* **2011**, *101*, 206-211.

(22) Kitano, S.; Hashimoto, K.; Kominami, H. *Catal. Today* **2011**, *164*, 404-409.

(23) Kominami, H.; Kohno, M.; Takada, Y.; Inoue, M.; Inui, T.; Kera, Y. *Ind. Eng. Chem. Res.* **1999**, *38*, 3925-3931.

(24) Kominami, H.; Oki, K.; Kohno, M.; Onoue, S.; Kera, Y.; Ohtani, B. *J. Mater. Chem.* **2001**, *11*, 604-609.

(25) Murakami, N.; Mahaney, P. O. O.; Abe, R.; Torimoto, T. B. Ohtani, *J. Phys. Chem. C* **2007**, *111*, 11927-11935.

(26) Nosaka, Y.; Yamashita, Y.; Fukuyama, H. *J. Phys. Chem. B* **1997**, *101*, 5822-5827.

(27) Hirakawa, T.; Nosaka, Y. *Langmuir* **2002**, *18*, 3247-3254.

(28) Hirakawa, T.; Nosaka, Y. *J. Phys. Chem. C* **2008**, *112*, 15818-15823.

(29) Nosaka, Y.; Takahashi, S.; Sakamoto, H.; Nosaka, A. *J. Phys. Chem. C* **2011**, *115*, 21283-21290.

(30) *Handbook of Chemistry and Physics*; Lide, D. R., Ed.; CRC Press, Inc.: Boca Raton, FL, 1993

(31) Torimoto, T.; Nakamura, N.; Ikeda, S.; Ohtani, B. *Phys. Chem. Chem. Phys.* **2002**, *4*, 5910-5914.

(32) Serpone, N.; Pelizzetti, E. Photocatalysis, Wiley, New York, 1989.

(33) Shlenskaya, I. V.; Efremenko, A. O.; Oleinikova, V. S.; Alimarin, P. I. *Russ. Chem. Bull.* **1969**, *18*, 1525.

(34) Bae, E.; Murakami, N.; Ohno, T. *J. Mol. Catal. A: Chem.* **2009**, *300*, 72-79.

(35) Murakami, N.; Kurihara, Y.; Tsubota, T.; Ohno, T. *J. Phys. Chem. C* **2009**, *113*, 3062-3069.

Figure captions

Figure 1. A) Rh K-edge XANES spectra of Rh foil, Rh_2O_3 and Rh^{3+}/TiO_2 samples. B) Enlargement of part A.

Figure 2. Fourier transforms (FT) of k^3-weighted Rh-K edge EXAFS spectra of Rh_2O_3 and Rh^{3+}/TiO_2 samples.

Figure 3. Time courses of photocurrent using a) Rh^{3+}/TiO_2 and b) bare TiO_2 electrodes under irradiation of visible light.

Figure 4. Current-potential curves of a) Rh^{3+}/TiO_2 and b) bare TiO_2 electrodes under dark in the presence of air.

Figure 5. Time courses of PA signals of a) Rh^{3+}/TiO_2 and b) bare TiO_2 samples under irradiation of visible light in the presence of N and ethanol. 2

Figure 6. Time courses of PA signals of a) Rh^{3+}/TiO_2 and b) bare TiO_2 samples under irradiation of UV light in the presence of air and ethanol.

Figure 7. Assumed schemes of electron transfers from Rh^{3+} to the conduction band of TiO_2 in Rh^{3+}/TiO_2 under irradiation of visible light: (A) indirect charge transfer and (B) direct charge transfer.

Figure 8. Diffuse reflection spectra of (A) bare and (B) Rh^{3+}-modified semiconductor oxide samples and emission spectra of visible and UV light.

Figure 9. Rate of CO formation for decomposition of acetone in gas phase under irradiation of visible light using Rh^{3+}-modified semiconductor samples.

Figure 10. Rate of CO_2 formation for decomposition of acetone in gas phase under irradiation of UV light using bare and Rh^{3+}-modified Ta_2O_5 samples.

Figure 11. Time courses of $O_2^{\bullet-}$ and H_2O_2 formed by Rh^{3+}/TiO_2 under irradiation of visible light.

Figure 12. Scheme of the working mechanism of the Rh/TiO_2 photocatalyst.

Table 1 Physical properties of various semiconductor samples.

Semiconductor	Conduction band potential / V *vs*. NHE	Band gap /eV	S_{BET} /m^2g^{-1}
Ta_2O_5	-1.0	4.0	50
TiO_2	-0.2	3.2	81
Nb_2O_5	0.0	3.4	250
SnO_2	0.5	3.5	30

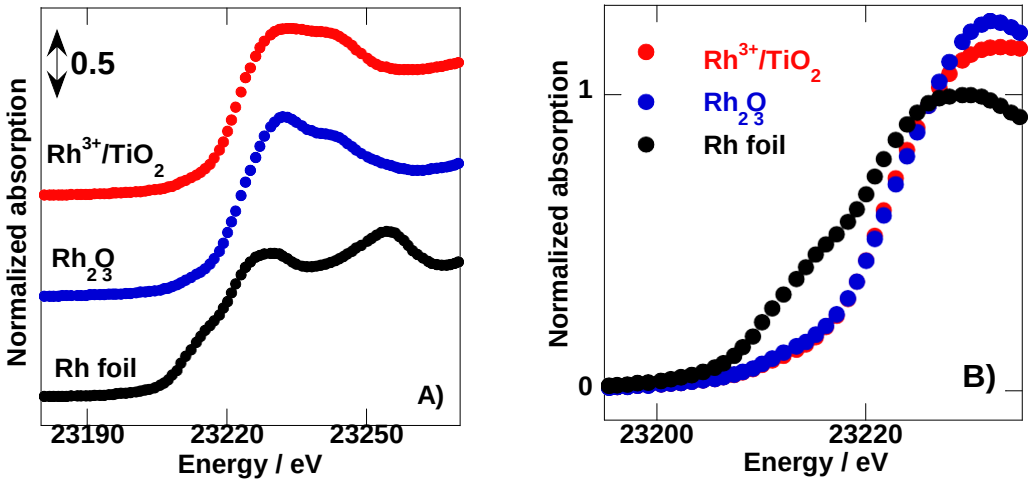

Figure 1. A) Rh-K edge EXAFS spectra of Rh2O3 and Rh3+/TiO2 samples.
B) Enlargement of part A.

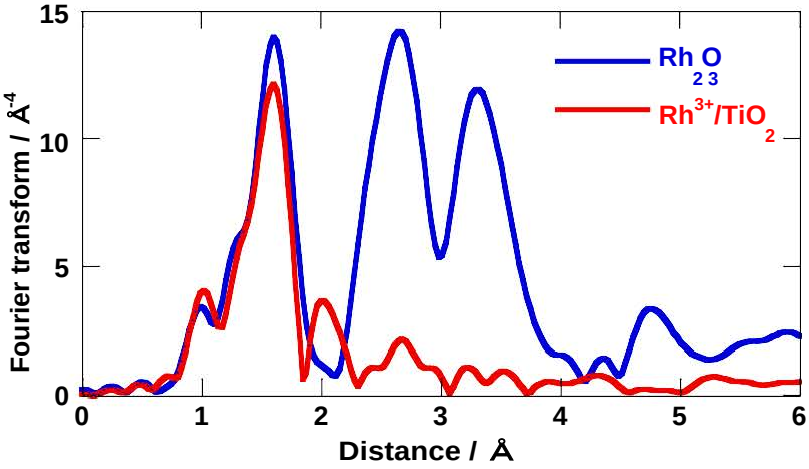

Figure 2. Fourier transforms (FT) of k^3-weighted Rh-K edge EXAFS spectra of Rh_2O_3 and Rh^{3+}/TiO_2 samples.

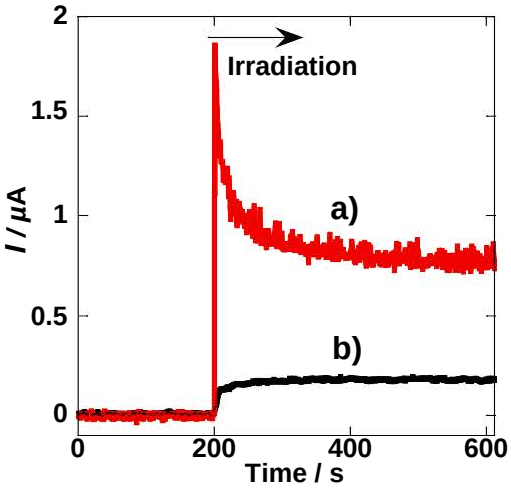

Figure 3. Time courses of photocurrent using a) Rh^{3+}/TiO_2 and b) bare TiO_2 electrodes under irradiation of visible light.

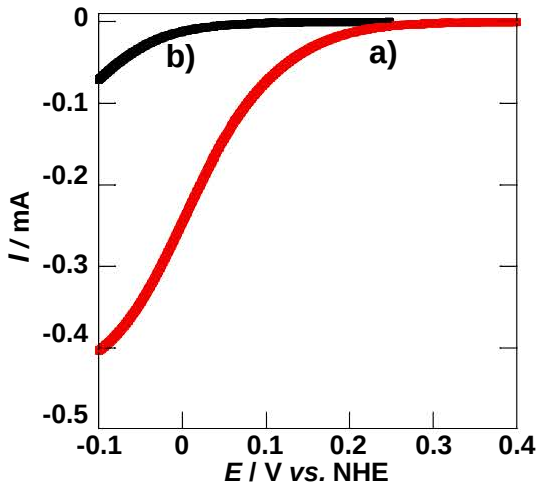

Figure 4. Current-potential curves of a) Rh^{3+}/TiO_2 and b) bare TiO_2 electrodes under dark in the presence of air.

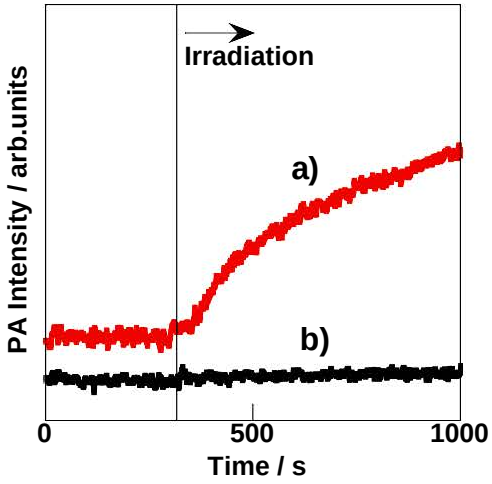

Figure 5. Time courses of PA signals of a) Rh^{3+}/TiO_2 and b) bare TiO_2 samples under irradiation of visible light in the presence of N_2 and ethanol.

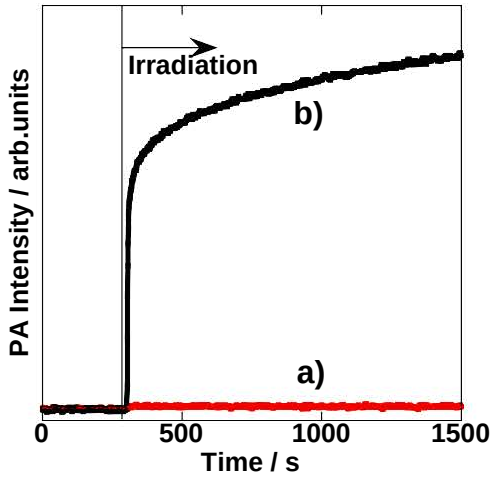

Figure 6. Time courses of PA signals of a) Rh3+/TiO2 and b) bare TiO2 samples under irradiation of UV light in the presence of air and ethanol.

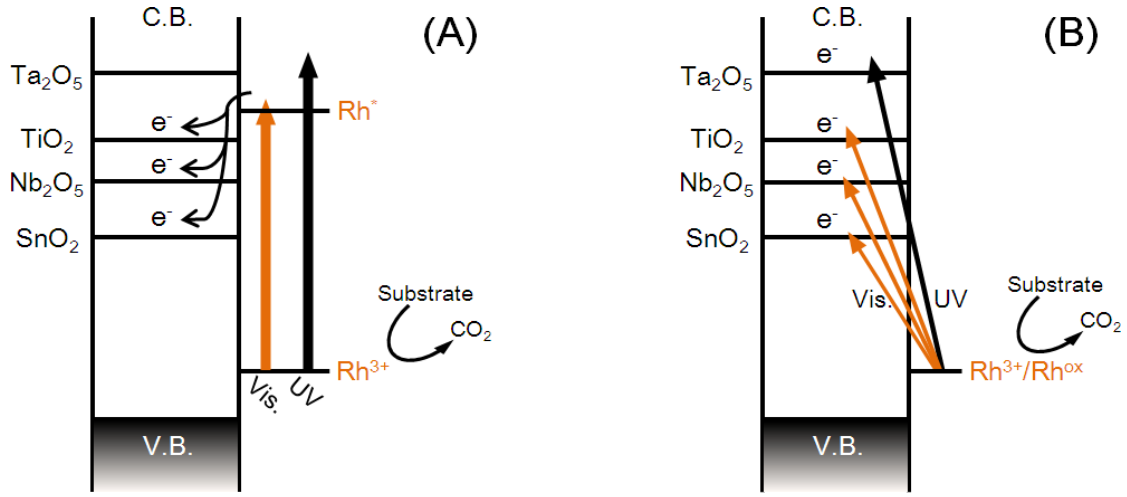

Figure 7. Assumed schemes of electron transfers from Rh^{3+} to the conduction band of TiO_2 in Rh^{3+}/TiO_2 under irradiation of visible light: (A) indirect charge transfer and (B) direct charge transfer.

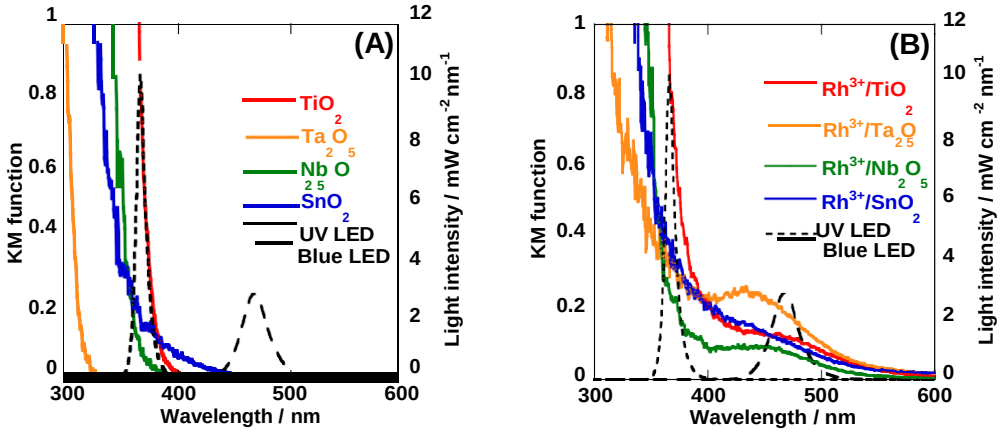

Figure 8. Diffuse reflection spectra of (A) bare and (B) Rh^{3+}-modified semiconductor oxide samples and emission spectra of visible and UV light.

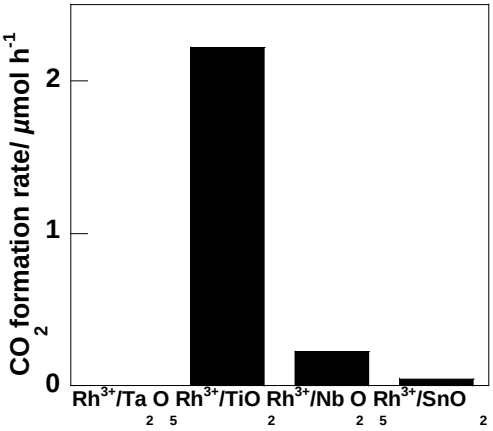

Figure 9. Rate of CO2 formation for decomposition of acetone in gas phase under irradiation of visible light using Rh^{3+}-modified semiconductor samples.

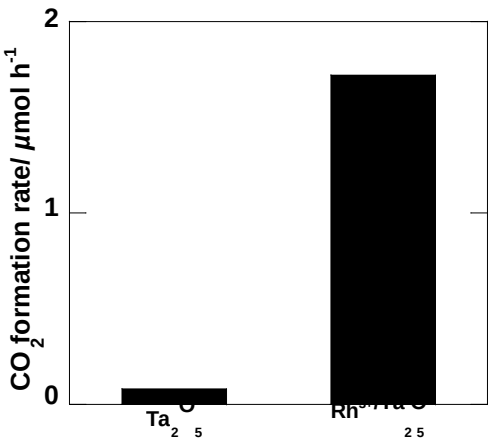

Figure 10. Rate of CO2 formation for decomposition of acetone in gas phase under irradiation of UV light using bare and Rh^{3+}-modified Ta_2O_5 samples.

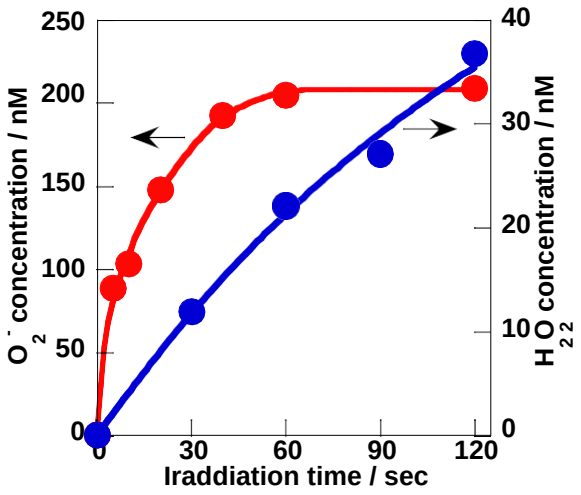

Figure 11. Time courses of $O_2^{\bullet-}$ and H_2O_2 formed by Rh^{3+}/TiO_2 under irradiation of visible light.

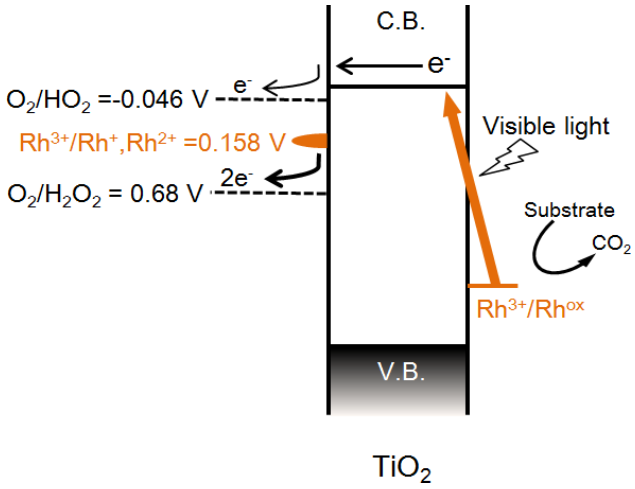

Figure 12. Scheme of the working mechanism of the Rh/TiO_2 photocatalyst.

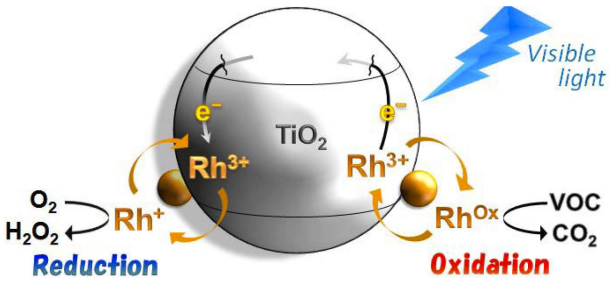
Visible
light
e⁻
e⁻
TiO2
Rh3+
Rh3+
O2
H2O2
Rh+
RhOx
VOC
CO2
Reduction
Oxidation